water

MDPI

Article

The Montellina Spring as an Example of Water Circulation in an Alpine DSGSD Context (NW Italy)

Domenico Antonio De Luca [1], Elena Cerino Abdin [2], Maria Gabriella Forno [1], Marco Gattiglio [1], Franco Gianotti [1] and Manuela Lasagna [1,*]

[1] Earth Sciences Department, Turin University, via Valperga Caluso 35, 10125 Torino, Italy; domenico.deluca@unito.it (D.A.D.L.); gabriella.forno@unito.it (M.G.F.); marco.gattiglio@unito.it (M.G.); franco.gianotti@unito.it (F.G.)

[2] Dipartimento di Ingegneria dell'Ambiente, del Territorio e delle Infrastrutture—DIATI, Politecnico di Torino, 10125 Torino, Italy; elena.cerino@polito.it

* Correspondence: manuela.lasagna@unito.it ; Tel.: +39-011-6705171

Received: 7 February 2019; Accepted: 2 April 2019; Published: 4 April 2019

Abstract: Alpine areas, with normally fissured bedrock outcrops, do not typically contain important hydrologic reservoirs, except for small aquifers located in Quaternary sediments. By contrast, mountainous areas affected by deep-seated gravitational slope deformations (DSGSD), especially if covered by glacial sediments, contain large aquifers and are consequently promising for water exploitation. This last geological setting is observed, for example, in the lower Dora Baltea Valley (near the confluence with the Renanchio Basin) in which the Montellina Spring is located and exhibits a very high discharge. A multidisciplinary approach (detailed geological survey of the bedrock and Quaternary cover, as well as hydrogeological research based on tracer tests, hydrochemical analyses, and water balance studies) was used, allowing for a reconstruction of the geological and hydrogeological setting of the investigated area, also considering its environmental implications. The consequent hydrogeological model derives from the coexistence of some factors. In detail, the thick glacial cover, widespread in the intermediate sector of the slope, represents an important aquifer with a slow groundwater flow to the spring. The buried glacial valley floor, hosting this cover, can convey the groundwater from the high Renanchio Basin zone towards the low sector. The loosened bedrock of the low sector, consequent to DSGSD phenomena, favors the concentration of groundwater along the contact with the underlying normal fissured bedrock outcropping at the base of the slope. Finally, the flow until the spring essentially takes place through N100° trend open fractures and trenches. Part of the Montellina Spring discharge is also fed by the low Renanchio Stream, as highlighted by fluorescein tests, essentially using NE-SW oriented open fractures on the bedrock. The results of the investigation on the Montellina Spring can provide some insight regarding the hydrological potential of other alpine areas with a similar geological setting.

Keywords: alpine spring; hydrogeological survey; DSGSD; glacial sediments; Western Alps; tracer tests

1. Introduction

Water is an essential resource, which becomes progressively more important with time considering the increase in water needs of populations and crops. Significant aquifers contained in alluvial plains and valley floors have often been exploited for many years, whereas smaller aquifers hosted in mountainous areas have, until now, been partially known and used [1]. Water reserves in mountainous areas are essentially located in extensive and thick sedimentary non-cohesive bodies (mainly debris, landslide and glacial deposits) and/or in large volumes of intensely fractured and loosened rocks involved in deep-seated gravitational slope deformation (DSGSD) areas [2–4].

Although rock masses affected by DSGSD are identified as important hydrogeological entities in mountain catchments, their characterization in terms of water availability and quality is limited to a few studies [5–7]. A high water availability particularly characterizes DSGSD areas covered by large bodies of glacial sediments, which are very common in alpine glacial valleys [5]. The significance of the water resources in DSGSD areas is suggested, for example, by some detailed hydrogeological research that highlights the connection between gravitational structures and water circulation [6]. The understanding of this connection has sometimes allowed the use of hydrogeological research for the identification of subsurface discontinuities in areas involved in gravitational phenomena [7]. Local investigations, such as the one proposed, can be critical to improving our general understanding of these geological complex systems.

The Montellina Spring is situated in a DSGSD area on the western side of the lower Dora Baltea Valley (Figure 1) [1]. The investigated area is located in the Eclogite Micaschist Complex (Astroalpine System, Sesia-Lanzo Zone), formed by a polycyclic basement with a mono-metamorphic cover (Scalaro Unit), both of which show regional foliation developed from alpine eclogite facies metamorphism [8–10].

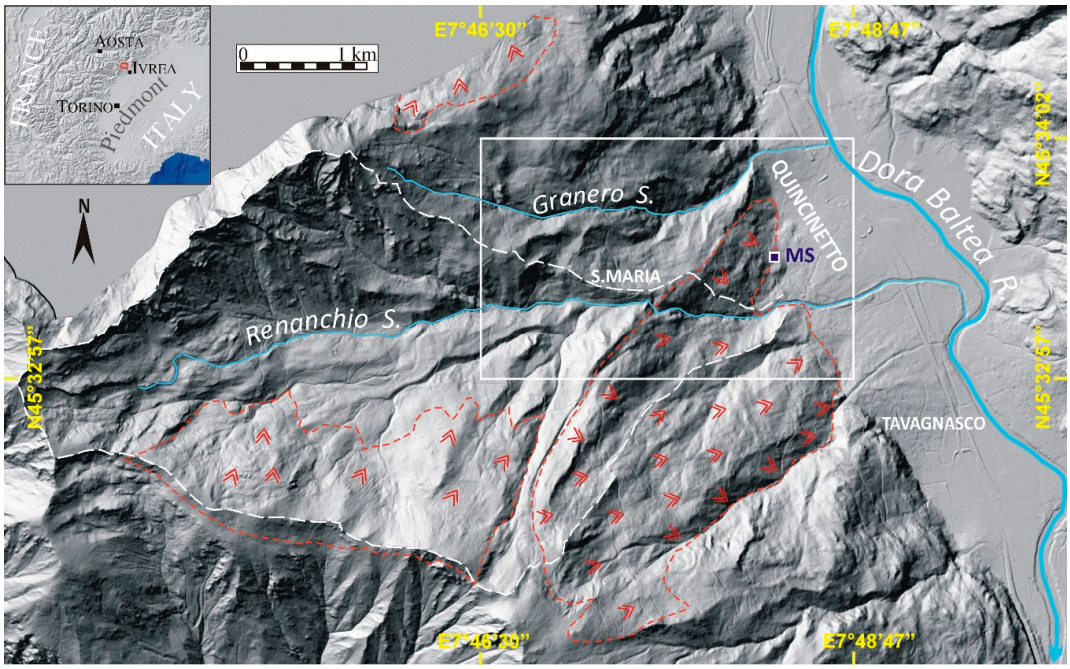

Figure 1. DTM reporting the right slope of Dora Riparia Valley in which the Montellina Spring (MS) is located and the Renanchio Basin. The red arrows represent the DSGSD areas. The white square indicates the investigated area.

The target of the study was to explain why Montellina Spring (MS) has relatively high discharge with respect to other alpine springs. For example, in the entire Turin Province, only 35 springs have a discharge higher than 10 L/s [1].

The Dora Baltea River basin, although characterized by an abundance of water due to the presence of high mountains and numerous glaciers, suffers from water deficits in terms of both quantity and quality, especially in summer and during periods of great tourist flow [11]. The main water supply consists of springs (about 78% of water extracted), sometimes with limited discharge (few L/s), while the remaining volume is taken from boreholes. Actually, there are about 1700 springs, of which 500 are used for drinking water purposes, resulting in around 60,000 cubic meters of water being available daily. Only the larger towns of the valley, located in the main valley floor, withdraw groundwater from wells drilled in alluvial aquifers [12]. More specifically, water resources no longer seem sufficient to cover requirements, and signs of possible conflict between different water users are becoming

evident [11]. Consequently, the study of the Montellina Spring can furnish a useful contribution to the knowledge of springs with high discharge in the DSGSD alpine context.

The research consisted of a multidisciplinary study that allowed for the reconstruction of the geological and hydrogeological setting of the investigated area. More specifically, the study comprised a detailed geological survey of the bedrock and Quaternary cover, and a hydrogeological investigation based on tracer tests, hydrochemical analyses, and water balance studies.

2. Location and Features of the Montellina Spring

MS is located at 375 m a.s.l. on the western slope of the low Dora Baltea Valley (Piedmont, NW Italy), near the Quincinetto Village (Figure 1). This spring is not developed at the base of the mountain, but is located approximately 100 m higher than the Dora Baltea Valley floor. Moreover, MS is located close (400 m) to the Renanchio Stream (a right tributary of the Dora Baltea River), suggesting a possible hydrogeological connection with the watercourse.

Due to its relatively high discharge, MS can be considered one of the springs for supplying drinking water with the highest discharge in the Turin Province [1,13,14]. In spite of its importance, few data are available for the possible interaction between groundwater and surface water (especially the Renanchio Stream) and the hydrogeological reasons that create conditions for its presence. Moreover, MS annual and inter-annual discharge data are not available because it is not possible to measure the MS discharge with continuous monitoring, due to the complexity of the spring water collection system.

A technical unpublished document [15] reports some information about MS and Renanchio Stream discharge, measured on a monthly basis in the period from February 2009 to April 2010 (Figure 2A). More recent data of MS discharge, from July to November 2011, are reported in a further technical document [16] (Figure 2B). The Renanchio Stream discharge was evaluated at an altitude of about 830 m a.s.l. with an NaCl tracer test, particularly with the instantaneous injection of a slug of NaCl into the watercourse. MS discharge was measured by combining discharge in the aqueduct pipes with an NaCl tracer test, through a slug injection in the overflow of the spring.

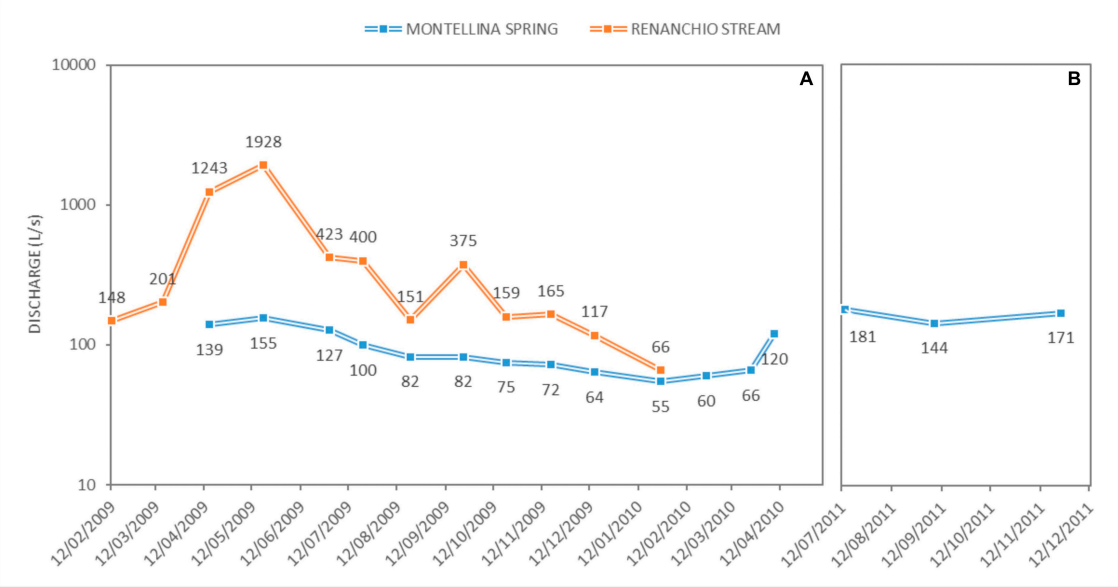

Figure 2. Montellina Spring and Renanchio Stream discharge ((**A**): modified from [15]; (**B**): modified from [16]).

These measures allow a comparison of MS and Renanchio Stream discharge that shows a common trend. However, MS discharge is always lower than discharge at Renanchio Stream. The discharge difference is higher with maximum flow in the springtime, especially in May, and decreases in summer

and autumn, with a minimum value of flow during winter. Moreover, MS discharge has a lower variability than the Renanchio Stream.

3. Methodology

The aim of this study is to clarify water circulation in the subsoil of the investigated area, which is also useful for improving our knowledge of other mountain springs in similar contexts. The synergy between geological surveys and hydrogeological methods was necessary to obtain the achieved results.

3.1. Geological Survey

The geological survey was directed to characterize outcropping bedrock both as lithology and degree of fracturing (from normally fractured to loosened), as well as to evaluate the sedimentological features of the various Quaternary sediments. The investigation also studied some typical gravitational morpho-structures of DSGSD, which involves both bedrock and surficial cover. This field survey, that brought the realization of a detailed geological map, was also combined with the interpretation of aerial photos, which were particularly useful for obtaining an overall view of the area and examining sectors that were difficult to access. The bedrock fracture setting and the porosity of Quaternary cover, as well as its permeability, are also well-investigated and used for the characterization of the spring supply, which was finalized to construct a hydrogeological model of the investigated area.

3.2. Hydrogeological Survey

The hydrogeological surveys consisted of five groundwater and surface water sampling campaigns; physical-chemical analyses, performed once per quarter for one year; evaluation of the hydrological balance of the Renanchio Basin; and the use of tracer tests. More specifically, sodium chloride (NaCl) tracer tests were performed for the evaluation of Renanchio Stream discharge, while fluorescein tracer tests were finalized for the evaluation of the rate at which the Renanchio Stream feeds MS. In order to facilitate the description of the hydrogeological survey results, the Renanchio Stream was subdivided into various stretches (Figure 3). The low Renanchio Stream (under 875 m a.s.l.) flows over a normally fractured or loosened bedrock. The middle Renanchio Stream (between 875 m a.s.l. and 975 m a.s.l.) is exclusively shaped in glacial marginal sediments without bedrock outcrops. The high Renanchio Stream (above 975 m a.s.l.) is shaped in the bedrock diffusely covered by glacial marginal sediments. The high and middle stretches are separated by the tracer injection point.

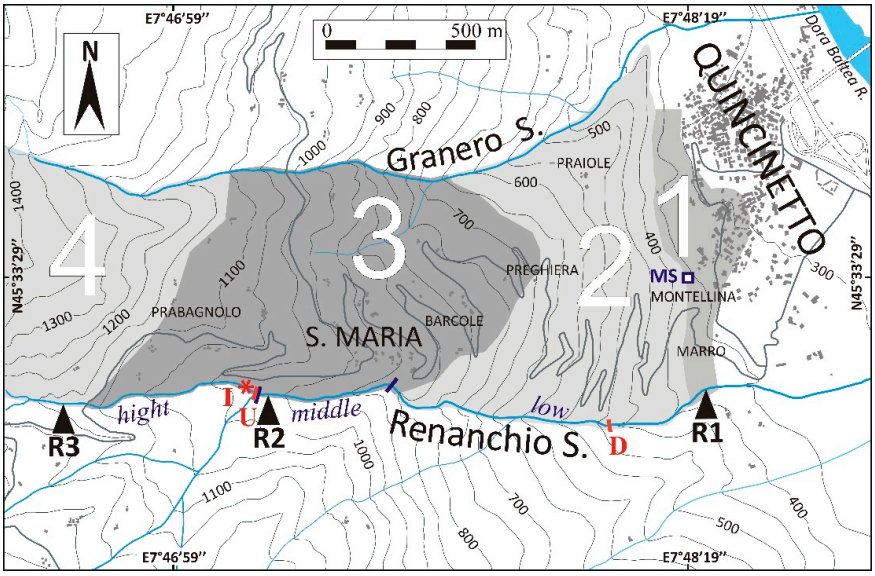

Figure 3. Location of the low, middle, and high stretches of the Renanchio Stream, reported in the text, and of the sectors of the investigated area. Sector **1** is essentially shaped in normally fissured bedrock;

sector **2** is prevalently shaped in loosened bedrock; sector **3** is characterized by a wide cover of glacial marginal sediments; sector **4** (only partly reported in the sketch) shows a wide distribution of highly fractured bedrock and glacial sediments. I: location of the fluorescein and NaCl injection; U: Renanchio Stream upstream section; D: Renanchio Stream downstream section. The water samples for chemical analyses are also represented: MS (Montellina Spring sample site), and R1, R2, and R3 (Renanchio Stream sample sites).

3.2.1. Water Sampling and Analyses

Five sampling campaigns were performed in November 2005, January 2006, February 2006, May 2006, and September 2006. In addition to MS, three sampling points were located along the Renanchio Stream bed, at altitudes of 375 m a.s.l. (R1 in the low stretch of the Renanchio Stream), 960 m a.s.l. (R2 in the middle stretch), and 1130 m a.s.l. (R3 in the high stretch) (Figure 3). The collection of water samples was performed using polyethylene bottles (0.5 L), previously washed. The water samples were preserved in a cool environment and immediately transferred to the laboratory for analyses.

Electrical conductivity and pH were measured in situ with a portable pH-meter and electrical conductivity-meter (Hanna Instruments). The temperature of MS and Renanchio Stream was measured with a field thermometer and compared to previous years.

Chemical analyses were performed in the Hydrochemical Laboratory of the Earth Science Department (Turin University) for water hydrochemical characterization. Alkalinity (HCO_3^-) was measured via a titration method using 0.1 N HCl. Major anions (NO_3^-, SO_4^{2-}, Cl^-) were determined using ion chromatography (Metrohms 709, 732, 733, 752, and 863). Major cations (Ca^{2+}, Mg^{2+}, Na^+, and K^+) were determined via ICP-AES (PerkinElmer, Waltham, MA, USA). Chemical data were treated with a Piper diagram [17]. This diagram permitted us to simultaneously compare a large number of water samples and allowed the definition of the hydrochemical facies of the water. Moreover, major ions were correlated with bivariate diagrams. More specifically, plots of HCO_3^- versus Ca^{2+} concentrations and HCO_3^- versus $Ca^{2+} + Mg^{2+}$ concentrations in the groundwater and surface water of the investigated area were reported.

3.2.2. Hydrologic Balance of the Renanchio Basin

A water balance was performed in the Renanchio Stream basin to evaluate the flow of water into and out of the hydrological system. The water balance equation can be expressed as follows:

$$P = Etr + Ie + R \quad (1)$$

where P is the precipitation, Etr is the evapotranspiration, Ie is the effective infiltration, and R is the runoff. The main assumption of the model considers that the net groundwater flow across the watershed boundaries is zero and, hence, the only inflow of water is P and the outflows are Etr, Ie, and R. The investigated area was divided into cells (250 m $\times$ 250 m), and for each cell, the parameters in the equation were evaluated.

The precipitation (P) and temperature (T) values were calculated starting from data that were recorded at four different rainfall stations located near the investigated area, at a distance of less than 8 km from MS. The data referred to a period of 13 years (1990–2002). Firstly, the inter-annual average precipitation and temperature values were evaluated for each station, from the P and T hourly data (Table 1).

Then, the correlation between elevation-precipitation and elevation-temperature was determined. These correlations show the variation of P and T values with the elevation. The precipitation and temperature values were then calculated for each cell according to the medium elevation of the cell.

Table 1. Inter-annual average precipitation and temperature values for each rainfall station.

Precipitation Station	Elevation (m)	Precipitation (mm/year)	Temperature (°C)
Borgofranco	337	909	10.5
Meugliano	650	1422	8.3
Pontboset	775	1250	9.2
Traversella	1165	1610	7.6

Evapotranspiration was evaluated according to the Turc formula [18]. The effective infiltration was calculated using the Cip method [19], considering the effective precipitation (Pe) and a potential infiltration coefficient defined as Cip, which is dependent on the type of outcropping rock and its permeability:

$$Ie = Pe \times Cip \quad (2)$$

The Cip values utilized for the main lithologies outcropping in the area are here reported: normally fissured bedrock 0.2, loosened bedrock 0.7, very fractured bedrock 0.5, and glacial marginal sediments 0.6 modified from [19].

Pe was calculated as the difference between the precipitation and evapotranspiration data.

The runoff was calculated according to the equation:

$$R = Pe - Ie \quad (3)$$

3.2.3. Tracer Tests for Streamflow Discharge and GW-SW Interactions Assessment

Measurements of streamflow discharge in successive cross-sections enable the determination of groundwater-surface water exchange by computing the differences in discharge between the cross-sections [20]. Streamflow discharge can be measured by various methods, including the velocity gauging method with a current meter [21], the gauging flumes method [22], or the dilution gauging method [23,24]. In this last method, a solute tracer is injected into the stream and the tracer breakthrough curves at successive cross-sections are recorded. The volumetric discharge can then be inferred from the measurements. Dilution gauging is especially used in mountainous streams where the irregular, boulder-laden cross-sections and the strong turbulence decrease the accuracy with which depth and velocity can be measured [25,26]. Therefore, three campaigns of tracer tests were conducted in this study, using dilution gauging. They refer to different Renanchio Stream flow regimes, and more specifically, Test 1 on 14 July 2011, Test 2 on 27 September 2011, and Test 3 on 24 November 2011.

Dilution gauging is commonly performed by either a constant flow injection or an instantaneous slug injection. The constant flow injection allows for a high accuracy, and it is used especially, and almost exclusively, for low flows (discharges less than approximately 0.1 $m^3\ s^{-1}$) [27]. On the other hand, the instantaneous slug injection can be used for higher discharges (flows up to 10 $m^3\ s^{-1}$ or greater) [27] and in more logistically complicated areas because the measuring equipment is very easy to move. Consequently, an instantaneous slug injection of NaCl and fluorescein was used for the three tracer campaigns.

NaCl Tracer Tests

Sodium chloride (NaCl) was used as a tracer because it meets all the criteria for a good tracer. NaCl is "chemically conservative" (i.e., it does not adsorb onto river sediments), has a high solubility in water, is relatively non-toxic, can be measured in the field indirectly with a conductivity metre, and is cheap and readily available [27,28]. For these reasons, NaCl (in ionic form) is the most frequently used chemical tracer and provides good results [29–33].

Three NaCl tracer tests were performed in the investigated area for the evaluation of Renanchio Stream discharge. Moreover, measurements of streamflow discharge in two cross-sections, defined as the upstream section at 970 m a.s.l. (U in middle Renanchio Stream) and downstream section at

475 m a.s.l. (D in low Renanchio Stream), allowed the determination of groundwater-surface water exchange (Figure 3). For discharge measurements, a mass of NaCl was dissolved in two barrels of stream water and mixed well. Then, the tests were performed with the instantaneous injection of the slug of NaCl (in ionic form) into the stream by inverting the barrels containing the tracer solution and the evaluation of the total mass of the tracer at a sampling cross-section located about one hundred metres downstream of the injection point. Particularly, a large mass (39 kg) of NaCl was used in Test 1 in the upstream section and 30 kg in the downstream section, because the stream had an elevated discharge caused by a high precipitation meteorological event that occurred in the days before the test. The mass of NaCl was 25 kg in the upstream section during Test 2 and Test 3, while it was 30 kg and 20 kg in the downstream section, respectively, for Test 2 and Test 3.

The basic principle is that the ionic NaCl concentration in the slug increases the natural water concentration; this increases the measured electrical conductivity (EC), which can be used as an index of the salt concentration. Over a wide range of concentrations, the EC is indeed linearly related to salt concentration [23,26,27,34] so that the EC response can be transformed into an ionic concentration of NaCl.

Measurements of EC were conducted in the sampling cross-section with a portable electrical conductivity-meter (Hanna Instruments). The elapsed time between EC measurements was 5 s. The EC values were transformed into concentration values using a calibration line, which was determined in the laboratory by detecting the variation in EC in the stream water after the addition of a certain amount of NaCl.

The equation for computing stream discharge is [23]

$$Q = \frac{V_0 \times C_0}{\int_0^\infty (C_t - C_b)\, dt} \quad (4)$$

where Q is the discharge of the stream in the measuring stretch, V_0 is the volume of the tracer solution injected into the stream, C_0 is the concentration of the tracer solution injected into the stream, C_t is the measured tracer concentration at a given time at the downstream sampling site, C_b is the background concentration of the stream, and dt is the time between two measures of EC in second (s).

The low and middle Renanchio Stream water losses (L) were evaluated using the difference between the measured stream discharge at the upstream section (QtU) and the stream discharge in the downstream section (QtD), according to the equation:

$$L = QtU - QtD \quad (5)$$

Fluorescein Tracer Tests

Sodium fluorescein ("uranine" or "fluorescein") tracer tests were conducted for the evaluation of the discharge of MS coming from the Renanchio Stream. Fluorescein is a fluorescent dye that has been widely used for measurements of discharge for surface water or groundwater studies in karst environments and for the determination of groundwater-surficial water (GW-SW) interactions [32,35–37]. This chemical compound has an acceptable environmental impact and it is easily detectable using a fluorometer [38–43]. Fluorescein has varying ranges of reactivity with different types of rocks [44,45], which must be considered prior to use.

Quantitative dye-tracer tests require an accurate measurement of the amount (mass) of tracer dye injected, the discharge from the spring during the test, and the concentration or total mass of tracer dye resurging from the aquifer. Quantitative dye-tracer tests are primarily used to obtain information about the time-of-travel and breakthrough characteristics of the tracer dye and to investigate flow properties [36].

At last, the analysis of the tracer recovery curve permits different information to be derived. The shape and magnitude of the dye-breakthrough curve are most influenced by: (1) amount of injected dye, (2) velocity and magnitude of the flow, (3) hydraulic properties of the flow path taken

by the tracer dye, and (4) other factors that affect mixing and dispersion of the tracer dye in the aquifer [46,47]. Tracer constituents in groundwater systems typically show an initial "breakthrough", which is an indication of the arrival of the tracer constituent. The "residence time" or travel time of the bulk of the tracer-constituent mass is typically indicated by the time from the beginning of the injection to the peak concentration of the tracer constituent [47,48]. Then, a sharp peak and rapidly receding concentrations can indicate little storage in the groundwater system. A broad peak and gradual decline of the receding concentrations can indicate slow groundwater velocities or ample storage capacity in the aquifer. Multiple peaks of the tracer-recovery curve can indicate multiple flow paths for tracer movement through the groundwater system, where the different flow paths have different residence times [49].

Three tracer tests were performed in this study by a slug injection of a known amount of fluorescein in the Renanchio Stream at 975 m a.s.l. (located between middle and high Renanchio Stream) previously weighted and diluted in the laboratory (Figure 3).

Because fluorescein is particularly photosensitive [36], during the transport to the investigated area, the fluorescein was kept away from light, in order to avoid photodegradation. The injected fluorescein mass was selected based on the Renanchio Stream flow regime. The mass was 3950 g in Test 1, 2000 g in Test 2, and 2950 g in Test 3. The fluorescein was continuously monitored at the MS at regular time intervals. The detection time interval was 1 h in the first tracer test, and was 15 min in the second and third tests. Measuring equipment included a flow-through field fluorometer (GGUN-FL30, Albilia) for the real-time measurement of the tracer concentration [50,51]. The location of the fluorometer in the spring remained unchanged for all three tracer tests. The fluorescein detection limit was 0.02 μg/L. The automatic field fluorometer permitted in-situ measurements of fluorescent dyes in water to be made. Moreover, the temporal resolution, precision, and accuracy are significantly enhanced compared to charcoal bags or water sampling [52]. Another advantage of in-situ measurement is the absence of transportation and analysis of bottled samples.

The mass of fluorescein recovered at the spring (Mr, g) was evaluated according to the equation [36,53]:

$$\mathrm{Mr} = \int_0^\infty \mathrm{C(t)Qs(t)dt}, \tag{6}$$

where C (t) is the measured dye concentration of the sample (g/l), Qs (t) is the discharge measured at the spring (L/s) in the same day, and dt is the time interval between two measures of fluorescein amount (s). The MS discharges used are reported in [15].

The discharge of the low and middle Renanchio Stream that feeds MS (QtUs, L/s) was evaluated using the following equation:

$$\mathrm{QtUs} = (\mathrm{Mr}/\mathrm{Mi}) \times \mathrm{QtU}, \tag{7}$$

where Mi is the mass (g) of fluorescein injected into the stream and QtU is the discharge in the upstream section of the middle Renanchio Stream.

The percentage of water that directly supplies MS fed by the low and middle Renanchio Stream (QtUs%) was calculated using the equation:

$$\mathrm{QtUs\%} = (\mathrm{QtUs} \times 100)/\mathrm{QtU} \tag{8}$$

Finally, the percentage of MS discharge that is directly fed from the low and middle Renanchio Stream (Qs%) was evaluated according to the equation:

$$\mathrm{Qs\%} = (\mathrm{QtUs} \times 100)/\mathrm{Qs} \tag{9}$$

4. Results

4.1. Results of the Geological Survey

The investigated area is located in the Dora Baltea Valley near its confluence with the Renanchio Stream (Figure 1). Different sectors of the slope can be distinguished: a steep sector located at the base of the slope that is characterized by normal-fractured bedrock that locally crops out (sector 1), a second steep sector with loosened bedrock involved in a wide DSGSD (sector 2), a third gently dipping sector that shows a thick cover of glacial sediment (sector 3), and a very extensive fourth sector that corresponds to the high Renanchio Valley partially involved in a DSGSD and covered by glacial sediments (sector 4) (Figure 3). MS is located near the permeability boundary between normal fissured bedrock forming sector 1 and loosened bedrock constituting sector 2.

4.1.1. Bedrock

The bedrock consists of a polycyclic metamorphic basement and a mono-metamorphic cover (Figure 4). The basement is mainly composed of coarse-grained micaschist. Medium-grained fengitic orthogneiss, several tens of metres in size, forms tabular bodies within the polycyclic micaschist, which occur parallel to the regional foliation trend. Smaller meta-aplite, eclogite, and glaucofanite bodies are also present.

Figure 4. Geological map of the Dora Baltea Valley slope comprising the Montellina Spring. (1) Eclogite micaschist and gneiss; (2) dolomitic marble; (3) loosened bedrock (essentially constituted by micaschist); (4) subglacial sediments; (5) glacial marginal sediments; (6) glacial marginal outwash and lacustrine sediments; (7) proglacial outwash sediments; (8) torrential and fluvial sediments; (9) landslide sediments; (10) debris; (11) cross-section trace represented in Figure 5; (12) foliation attitude; (13) moraines; (14) glacial striae; (15) buried glacial valley floor; (16) minor scarps; (17) trenches; (18) landslide niches; (19) alluvial fans; (20) minor springs; (21) Montellina Spring. The sectors **1, 2, 3,** and **4**, as indicated in Figure 3, are also reported.

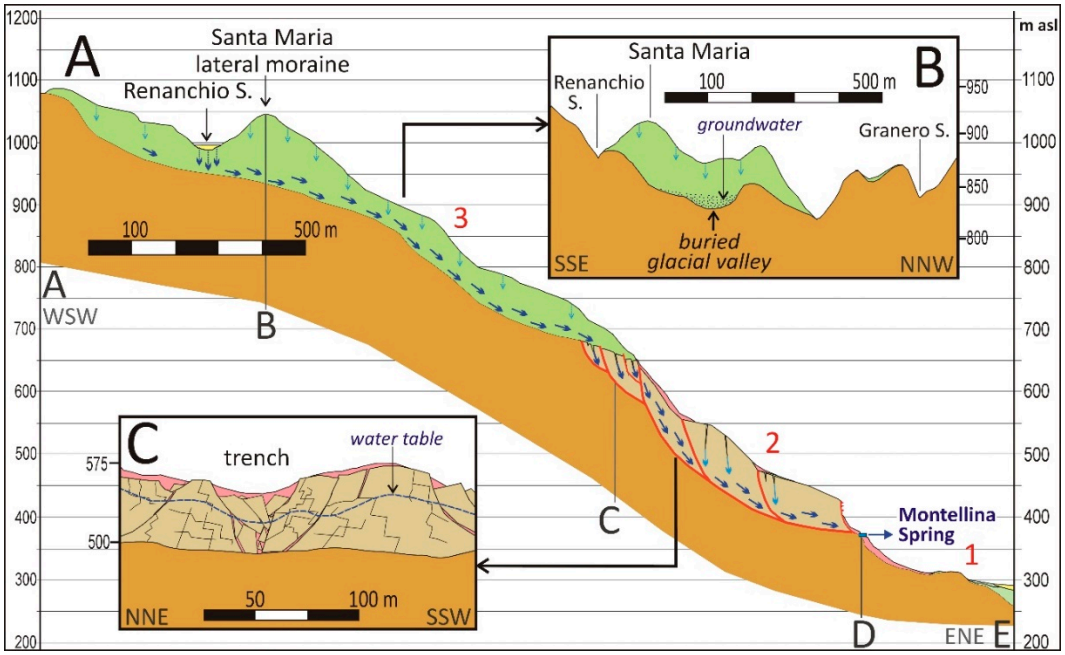

Figure 5. Schematic cross-sections (see the legend in Figure 4). (**A**) The water of the high Renanchio Stream (upstream of the fluorescein injection) infiltrates the glacial marginal sediments of sector 3 (upstream of the Santa Maria lateral moraine) and essentially flows through the buried glacial valley. This water flow continues in the loosened rocks of sector 2, supplied by the water infiltrating in the open fractures, feeding MS. (**B**) Cross-section of the buried glacial valley, covered by glacial deposits, in which groundwater is conveyed. (**C**) Detail of the loosened rocks that transfer the groundwater of the buried glacial valley to MS, especially through longitudinal trenches.

The mono-metamorphic cover is composed of fine-grained quartz micaschist, with varying carbonate content, interlayered with decimetric bodies of white quartzite. These lithologies are overlain by fengitic grey marble, dolomitic white marble, and less widespread calcschist. The marble mainly crops out in the sector 2, forming levels up to a decametric size. The marble layers show a more limited and discontinuous distribution and a smaller thickness (few meters) compared to that described in the literature [14].

The regional foliation dips towards the S and E and is weakly deformed by two sets of post-regional foliation folds that trend NW-SE and NE-SW, respectively. Several fracture systems, variably open, have been recognized in the investigated area. Fracture system **1** is the best developed and shows extensional kinematic indicators. The fracture surfaces, striking approximately E-W and dipping both N and S, are characterized by gouge up to a decimetric size. Open fractures have been recognized upstream of MS and assigned to this system. Fracture system **2** has steeply inclined detachment surfaces that trend SSW-NNE or SW-NE and dip to the ESE or SE, which favors the formation of minor scarps according to the trend of the main valley slope (Figure 6). The fractures of system **3** strike N-S and dip E, with kinematic indicators indicating right- and left-lateral movements. Fractures of system **4** trend NW-SE and dip NE, favoring the collapse phenomena, such as those in sector 1, which have given rise to landslide accumulations around Molino (Figure 4).

This variety of fracture systems is connected to a deep-seated gravitational slope deformation phenomenon (DSGSD) that greatly loosens the bedrock, giving it a high permeability (Figure 6). The fracturing is particularly well-developed in sector 2, where normally fractured rock volumes with evidence of glacial shaping ("roches moutonnées") that exhibit dimensions of hundreds of square metres are also preserved, especially in the Praiole-Preghiera ridge (Figure 4). The distribution and trend of glacial striae support the exaration of these reliefs by the main Dora Baltea Glacier, suggesting the shaping of the low strip of the slope by this glacier (see Figure 7A).

Figure 6. Loosened rocks outcropping in sector 2 characterized by high permeability due to fractures.

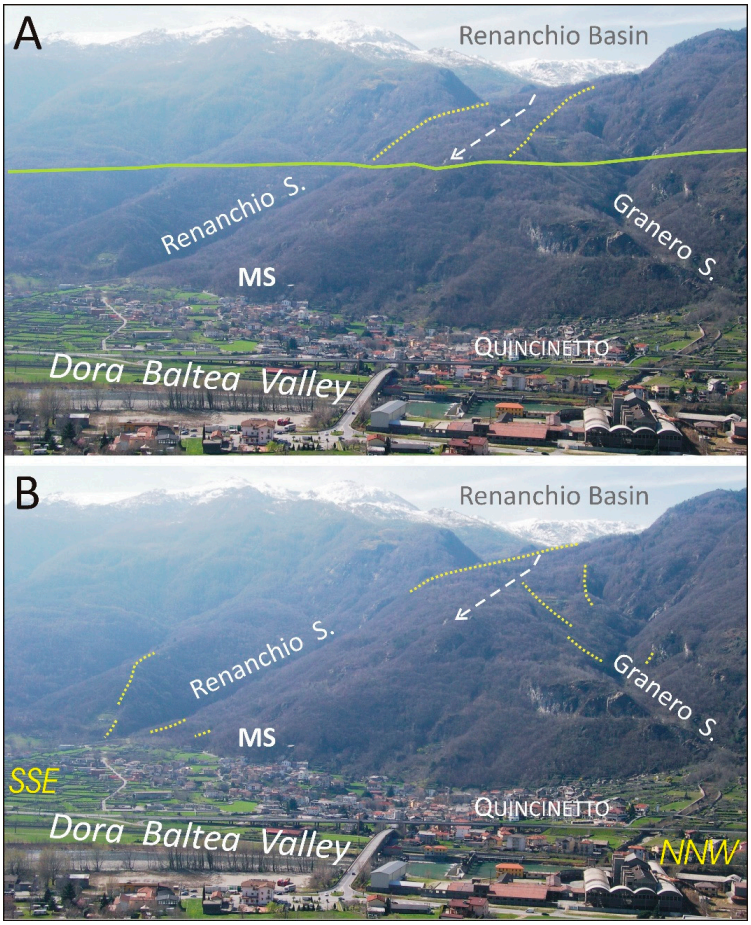

Figure 7. Location of the Montellina Spring (MS) along the right slope of the Dora Baltea Valley during LGM (**A**) and Lateglacial (**B**). (**A**) Downstream of the high Renanchio Basin (sector 4), clearly shaped by the Renanchio Glacier, a buried glacial valley floor (white arrow) is assumed, covered by the Renanchio Glacier sediments forming large lateral moraines (yellow lines) (sector 3). This valley floor ends at approximately 675 m, where the confluence of the tributary glacier with the main Dora Baltea Glacier was likely located (green line). The lower strip of the slope (under the green line) (sectors 2 and 1) is essentially shaped by the Dora Baltea Glacier. (**B**) The retreat of the main Dora Baltea Glacier during the Lateglacial favors the subsequent advance of minor lateral glaciers (Renanchio and Granero glaciers) into the current incisions until the main valley floor.

4.1.2. Quaternary Succession

The Quaternary succession covers most of the investigated area, comprising glacial and gravitational sediments. Subglacial sediments form a discontinuous band in the low slope, locally cropping out along the Praiole and Moia ridges in sector 3, as well as near the Quincinetto village in sector 1. They directly cover the rocky slope, with a visible thickness up to several metres (Figure 4). The subglacial cover essentially consists of overconsolidated silt with few pebbles, containing centimeter-scale smooth and striated clasts. These sediments, essentially gray in colour, are massive or show an NE dipping bedding, according to the slope. The petrographic composition of gravel, including clasts from local units (eclogite micaschist, eclogite, gneiss, marble, and quartzite) and exotic clasts (not eclogite micaschist, gneiss, prasinite, and serpentinite), suggests a supply from the main Dora Baltea Glacier. Its permeability for porosity is very low.

Glacial marginal sediments, by comparison, extensively cover the wide sector 3 between S. Maria and Praiole, and also locally outcrop in sectors 1 and 2 (near Marro) (Figure 4). These sediments range from ten to over thirty metres along the middle Renanchio Stream bed. They consist of variably sized clasts (from a decimeter-scale to greater than ten metres), which are mostly faceted with rounded edges in a scarce sandy-silty matrix, with normal consolidation and medium permeability for porosity ($k = 10^{-4} \div 10^{-6}$ m/s depending on the matrix grain size) (Figure 8). These sediments only include local clasts (eclogite micaschist, eclogite, gneiss, marble, and quartzite), suggesting a sediment supply from the Renanchio Glacier.

Figure 8. Typical features of glacial marginal sediments outcropping in sector 3, characterized by medium permeability for porosity.

The glacial marginal sediments form a set of asymmetric ridges elongated in an average WSW-ENE trend, regarded as lateral moraines (Figure 4). These moraines are separated by incisions that can be interpreted as spillway channels partially filled by outwash sediments (not represented in the geological map because of their small extent). Most large moraines are located in the wide area comprised between the current Renanchio and Granero streams (sector 3), whereas smaller moraines are located along the low Renanchio and Granero streams (sectors 2 and 1).

The wide distribution of glacial marginal sediments and the trend of the reported large moraines (sector 3) suggest that these sediments fill a WSW-ENE glacial valley floor, located north of the Santa Maria-Preghiera ridge (reported as 15 in Figure 4). This incision, now buried, shows a WSW-ENE trend different with respect to the current, essentially W-E, tributary watercourses. The large moraines

and the supposed buried valley floor abruptly end at approximately 675 m a.s.l. and do not continue in sectors 2 and 1 (Figure 7), which are mainly shaped in the bedrock.

The great thickness of the glacial marginal sediments forming the large moraines (which does not allow for the outcropping of bedrock in the entire sector 3) also implies that the buried glacial valley floor was deeper than the current Renanchio incision shaped in the bedrock (see Figure 5B).

The wide distribution and preservation of the glacial sediments, as well as their weak weathering, support an age ranging from the Last Glacial Maximum (LGM) to the early stages of Lateglacial. Therefore, it is possible to hypothesize that the Renanchio Basin, during the LMG, hosted a wide glacier (Renanchio Glacier) responsible for the shaping both in the high basin, which preserves the typical glacial morphology and sediments, and in the low basin, where the buried valley floor (filled by moraines) is reported. In comparison, the glacial landforms of the high Renanchio Basin (sector 4) show continuity with the large moraines (sector 3), and these last landforms do not continue in the low slope (sectors 2 and 1). The distribution of subglacial sediments of the Dora Baltea Glacier in sectors 2 and 1 suggests that these sediments were exclusively supplied by the main glacier, and therefore, the confluence between the two glaciers during the second part of LGM was at approximately 675 m a.s.l. (Figure 7A).

The presence of small moraines in sectors 1 and 2, localized along the low current incisions of Renanchio and Granero streams, suggests that during the Lateglacial, small glacial tongues survived in the Renanchio Basin, after the retreat of the Dora Baltea Glacier, almost reaching the present main valley floor (Figure 7B).

Landslide deposits are also very common in the investigated area. They form a continuous cover in sector 1 (near Molino) (Figure 4). These sediments consist of angular clasts with various sizes of local rocks (eclogite micaschist, eclogite, marble, and quartzite) in a scarce silty-sandy matrix, responsible for the high permeability for porosity. The clasts are very large (up to 1000 m^3) at the distal edge of the accumulations near the Quincinetto village. These large boulders can often be mistaken as bedrock outcrops.

These sediments form convex, adjacent, highly dipping landslide accumulations that are separated by incisions hosting small springs. The detachment surfaces are visible W of the accumulations, along a relatively continuous rocky wall that has an NW-SE trend (conditioned by fracture system **4**). The landslide accumulations involve the loosened bedrock (eclogite micaschist) and locally (northern landslide body), its subglacial cover.

Finally, wide sectors at the base of the scarps are covered by debris, composed of angular clasts that are relatively constant in size (from centimetres to decimetres), without matrix, with high permeability. MS develops into the debris, at the boundary with a landslide accumulation.

4.1.3. DSGSD Morpho-Structures

The setting of sector 2, immediately upstream of MS, is strictly conditioned by numerous open fractures and trenches, with a width that ranges from centimetres to several metres, and minor scarps, showing a height of several metres (Figure 4). These structures fully change the setting of the bedrock, which assumes a scarce consistence and a high permeability due to fractures (Figure 6). The loosened rocks are part of a wide DSGSD that is prevalently located S of the Renanchio Stream (Figure 1). These loosened rocks cover the normally fractured bedrock that crops out in sector 1. The fracturing also favors the formation of detachment niches, multiple metres high, that are responsible for the deposition of landslide sediments and debris.

The N100° trend trenches along the DSGSD fracture system **1**, particularly developed in sector 2 upstream of MS, contribute to the MS feeding (Figure 4). They are several metres wide and cross-cut the glacial sediments and landforms (i.e., the "roches moutonnées").

Some SW-NE multiple metres high minor scarps, along the DSGSD fracture system 4, also involve the normal fissured bedrock, as is visible in the Renanchio Stream incision. They, located in sector 2

downstream of S. Maria, are likely responsible for the connection between the watercourse and MS (Figure 9).

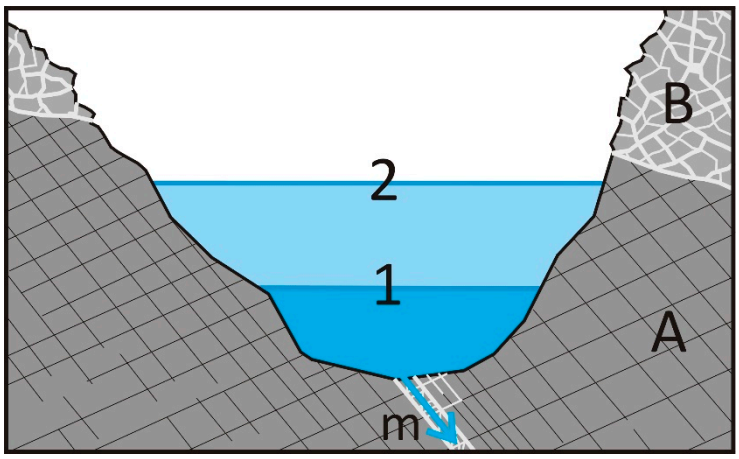

Figure 9. Schematic cross-section along the low Renanchio Stream, downstream of S. Maria: (**A**) Normally fractured rocks; (**B**) loosened bedrock. The Renanchio Stream supplies little MS both in low level 1 (during dry season) and in high level 2 (during flood) using some SW-NE minor scarps (m).

4.2. Hydrogeological Survey

4.2.1. Physical-Chemical Analyses

The results of chemical analyses indicate that the following relationship in the abundances of cations and anions was generally observed for all samples (Table 2): $HCO_3^- > SO_4^{2-} > NO_3^- > Cl^-$ and $Ca^{2+} > Mg^{2+} > Na^+ > K^+$.

Table 2. Results of the physical-chemical analyses performed in the Montellina Spring sample (MS) and Renanchio Stream samples (R1, R2, and R3). Sampling campaigns are referred to: November 2005 (A), January 2006 (B), February 2006 (C), May 2006 (D), and September 2006 (E); e% represents the accuracy of the result, quantified by calculating the percent error.

	Sampling Campaign	Ca^{2+} mg/l	Mg^{2+} mg/l	Na^+ mg/l	K^+ mg/l	Cl^- mg/l	SO_4^{2-} mg/l	HCO_3^- mg/l	NO_3^- mg/l	Electrical Conductivity (µS/cm)	pH	e%
MS	A	15.09	3.14	1.51	1.11	0.73	11.11	52.48	2.96	105	7.4	−2.4
	B	17.78	2.56	1.64	1.09	0.82	13.48	54.92	3.42	116	8.5	−2.5
	C	17.43	2.82	1.66	1.06	0.79	12.73	56.02	3.14	119	8.1	−2.2
	D	16.26	2.72	1.28	0.78	0.64	11.72	49.91	3.19	108	8.3	−0.9
	E	17.14	4.11	1.63	0.79	0.52	14.09	58.21	2.73	118	8.3	−0.8
R1	A	8.34	2.97	1.16	0.50	0.48	4.93	33.44	2.85	69	7.5	0.9
	B	13.88	1.72	1.35	0.45	0.64	6.33	43.93	3.66	90	7.6	−1.3
	C	13.13	1.92	1.33	0.49	0.64	6.29	43.45	3.20	85	7.5	−1.6
	D	9.23	0.48	0.79	0.44	0.42	4.13	25.14	3.34	57	7.4	−1.6
	E	14.36	2.60	1.33	0.59	0.53	6.42	48.21	2.48	94	8.2	1.3
R2	A	6.73	4.05	1.15	10.82	9.05	4.63	33.44	3.07	84	7.5	2.4
	B	12.60	2.01	1.36	0.49	0.73	5.74	40.64	3.48	85	7.7	0.2
	C	12.81	2.11	1.34	0.64	0.82	5.64	44.67	3.43	88	7.4	2.2
	D	9.28	1.04	0.74	0.49	0.42	4.14	29.90	3.14	57	7.4	−3.6
	E	12.94	1.02	1.21	0.52	0.48	5.86	43.45	2.69	86	8.1	−0.5
R3	A	8.02	3.24	0.99	0.55	0.46	4.89	36.00	2.73	69	7.5	−1.7
	B	12.23	2.34	1.04	0.38	0.41	5.38	41.37	3.32	80	7.6	0.2
	C	8.40	0.81	0.65	0.40	0.35	4.10	25.99	3.07	53	7.7	−4.2
	E	11.77	1.78	1.00	0.43	0.31	5.56	42.71	2.34	75	8.2	−4.5

The analyses for the MS showed constant hydrochemical values over time, whereas the analyses for the Renanchio Stream (R1, R2, and R3) showed values that were more variable. The main variability

regarded HCO_3^- that varied between 49.9 and 58.2 mg/L in MS samples, whereas it varied between 25.1 and 48.2 mg/L in the Renanchio Stream samples (25.1–48.2 mg/L in R1, 29.9–44.7 mg/L in R2, 26.0–42.7 mg/L in R3).

The electrical conductivity generally showed a value ranging between 57 and 90 µS/cm in the stream and higher values, between 105 and 119 µS/cm, in the MS.

Temperature in MS ranged between 8.9 °C and 10.0 °C, with an average value of 9.6 °C. The Renanchio Stream showed a higher variability both along the stream course and during the year (Table 3). More specifically, the stream temperature ranged between 5.4 °C in March 2009 and 15.3 °C in July 2011. Moreover, the temperature also varied in the same day, due to the altitude of the measurement. For example, the Renanchio Stream temperature increased by 2 °C between an altitude of 970 m a.s.l and 475 m a.s.l. on 14 July 2011, and by 1.6 °C between 1013 m a.s.l and 487 m a.s.l. on 3 October 2018.

Table 3. Temperature data referred to Montellina Spring and Renanchio Stream: ** measures from [14], * measures conducted during the tracer tests, and ° data from our other research. Data are related to punctual temperature measures, and measures conducted at time intervals (registered with a datalogger).

Location	Date/Time Period	Temperature (°C)
Renanchio Stream (altitude 450 m a.s.l.) **	16/03/2009	5.4
Renanchio Stream (altitude 970 m a.s.l.) *	14/07/2011	13.3
Renanchio Stream (altitude 475 m a.s.l.) *	14/07/2011	15.3
Renanchio Stream (altitude 1475 m a.s.l.) °	18/10/2017	8.6
Renanchio Stream (altitude 1013 m a.s.l.) °	03/10/2018	9.5
Renanchio Stream (altitude 965 m a.s.l.) °	03/10/2018	9.5
Montellina Spring °	25/01/2007–19/05/2007	10.0
Montellina Spring **	16/03/2009	9.8
Montellina Spring *	27/09/2011–07/11/2011	8.9
Montellina Spring °	18/10/2017	9.7
Montellina Spring °	03/10/2018	9.6

The presence of a quite constant water chemistry and temperature of MS is probably due to the presence of a large aquifer in the porous deposits, so as to allow homogenization of the chemical composition of groundwater throughout the year. The analysis of major ions using a Piper diagram (Figure 10) shows that groundwater and surface water samples belong to the Ca-Mg-HCO_3 facies. The prevalence of these ions can suggest that most of the water in the investigated area had limited exchange with the surrounding porous medium. A comparison of MS and Renanchio Stream water ions, using scatter plots, highlights a strong correlation (coefficient of correlation $R^2 = 0.94$) between HCO_3^- and Ca^{2+}, which could be related to the presence of marble in the area (Figure 11). The correlation further increases if Ca^{2+} and Mg^{2+} are considered ($R^2 = 0.97$), probably due to the dolomitic origin of some marbles.

Moreover, the MS water shows a higher ion concentration than Renanchio S. water; however, the ratio between $Ca^{2+} + Mg^{2+}$ and HCO_3^- remains almost constant. It represents clear evidence of a connection between surface water and groundwater.

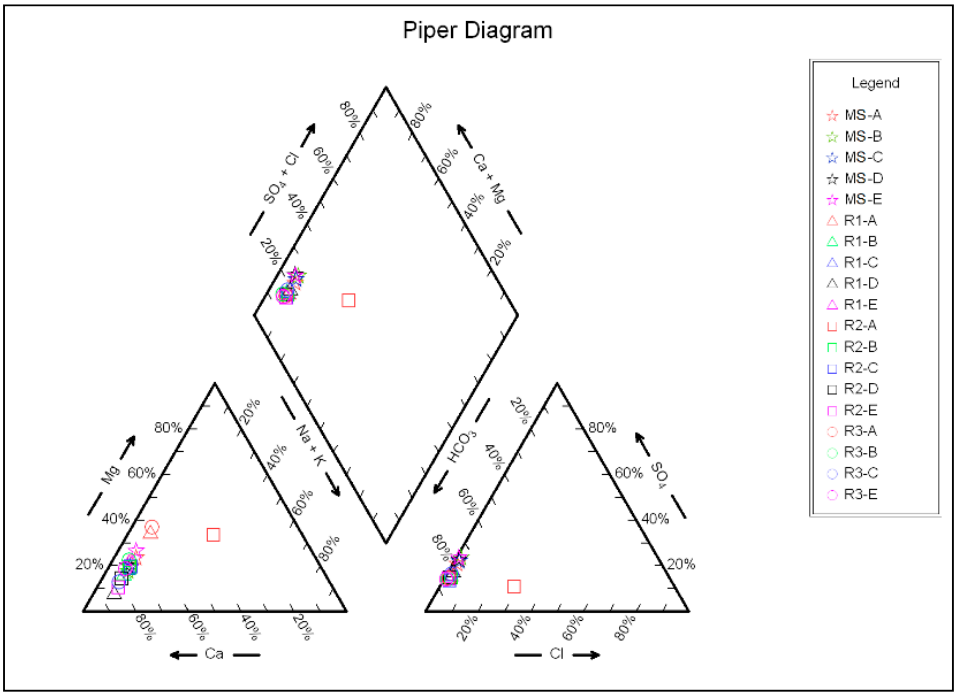

Figure 10. Piper diagram, including all sampled waters in the four sampling campaigns. The samples are referred to in Table 2. The apexes of the cation ternary plot are calcium, magnesium, and sodium plus potassium. The apexes of the anion plot are sulphate, chloride, and carbonate plus hydrogen carbonate.

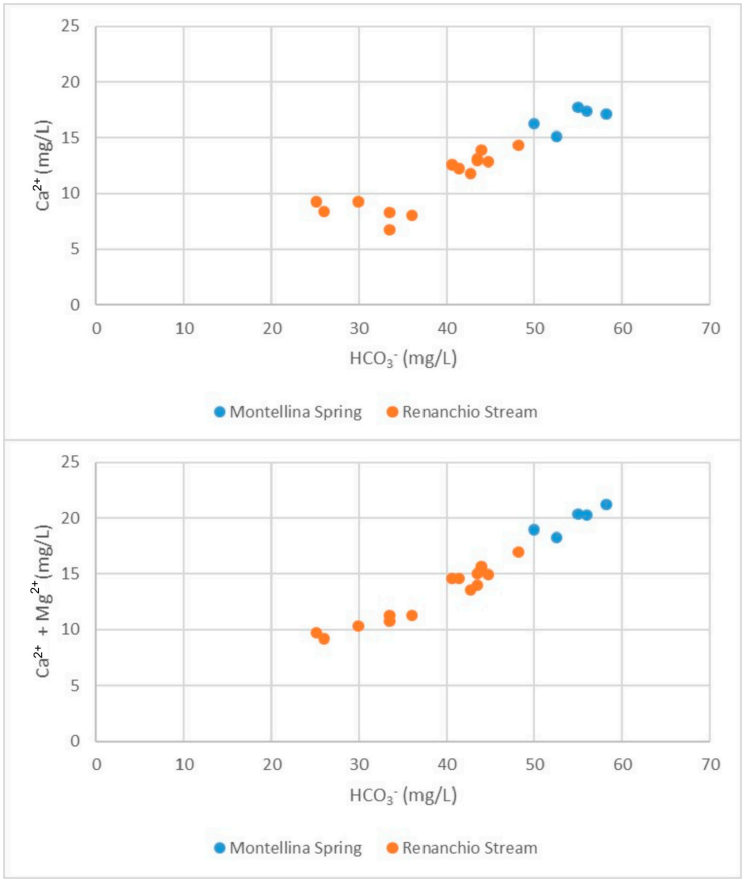

Figure 11. Plot of HCO_3^- versus Ca^{2+} concentrations and HCO_3^- versus Ca^{2+} + Mg^{2+} concentrations in the groundwater and surface water of the investigated area.

4.2.2. Hydrologic Balance

The results of the hydrologic balance for the Renanchio Basin referred to a period between 1990 and 2002 (Table 4). All of the parameters of the hydrologic balance are an "estimation" because they were mathematically evaluated and not directly measured in the field.

Table 4. Main annual parameters of the hydrologic balance of the Renanchio Basin.

Parameter	(Mm^3/y)
Precipitation	34.2
Evapotranspiration	9.4
Effective infiltration	11.8
Runoff	13

The overall annual MS discharge (2.8 Mm^3/y referred to the period April 2009–March 2010) represents approximately 24% of the effective infiltration in the Renanchio Basin area. Thus, according to the balance, the effective infiltration characterizing the basin is sufficient to supply MS.

4.2.3. Results of Tracer Tests

NaCl Tracer Tests

NaCl tracer tests were used to evaluate the stream discharge in the upstream section (QtU in the middle Renanchio Stream) and in the downstream section (QtD in the low Renanchio Stream), and the possible Renanchio Stream losses (L) between the upstream section and downstream section.

The results of these tests, performed during base and flood flows of the Renanchio Stream, show a higher discharge in the upstream section for all three surveys. More specifically, QtU was 1493 L/s in Test 1, 133 L/s in Test 2, and 353 L/s in Test 3. QtD was 1104 L/s, 102 L/s, and 312 L/s, respectively, in the three surveys. Thus, the losses (L) in the low and middle Renanchio Stream were evaluated as 389 L/s, 31 L/s, and 41 L/s, respectively, in Test 1, Test 2, and Test 3 (Figure 12). Consequently, a discharge loss of about 26% of the streamflow in Test 1, 23% in Test 2, and 11% in Test 3 can be estimated, relatively not influenced by very different discharge of the watercourse.

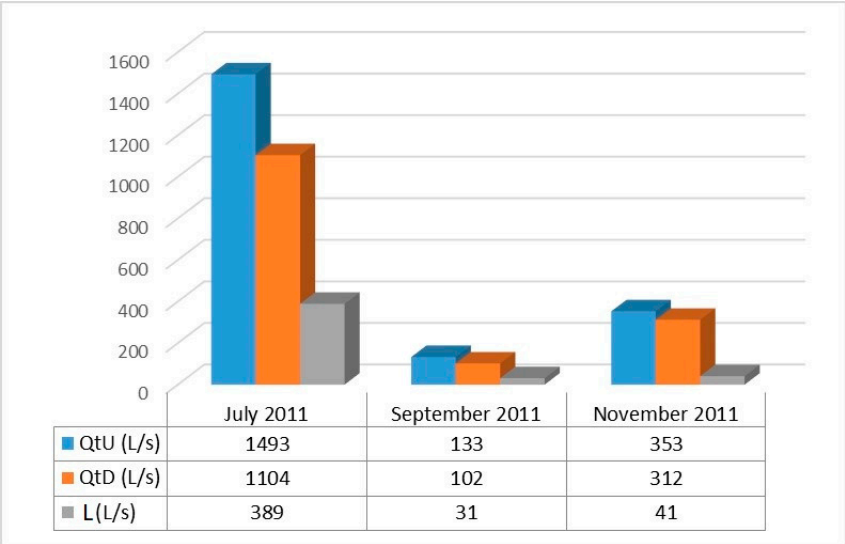

Figure 12. Comparison of the Renanchio Stream discharge in the upstream section (QtU) and downstream section (QtD) and losses (L) between the upstream section and the downstream section, in the three surveys (Test 1 in July 2011, Test 2 in September 2011, and Test 3 in November 2011).

Fluorescein Tracer Tests

Fluorescein tracer test results produced tracer recovery curves with an asymmetric trend, characterized by a quick-flow response in all three tests (Figure 13). More specifically, the dye breakthrough curves show a rapid arrival of the dye to the spring, indicating a little storage in the groundwater system before the arrival of spring, a single peak, and a gradual decline of the receding concentrations.

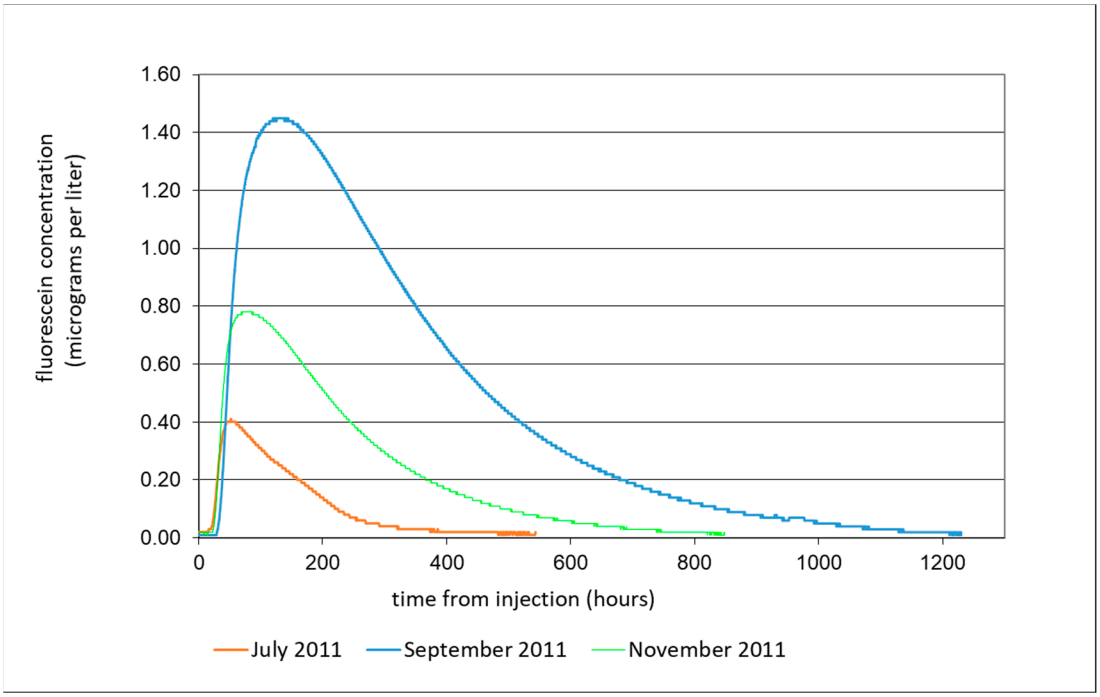

Figure 13. Dye breakthrough curves for the three fluorescein tracer tests performed.

The results of the fluorescein tracer tests (Table 5) indicate that in Test 1, the first fluorescein arrival at spring was 16 h after injection, and a peak concentration of 0.41 µg/L was measured 52 h after injection. Concentrations fell below the limit of detection within 22 days after injection. The mass of fluorescein (Mr) that had reached the Montellina Spring, obtained using Equation (6), was equal to 38.086 g. Thus, the amount of water from the Renanchio Stream that feeds MS (QtUs) was calculated to be 14.4 L/s, which corresponds to less than 1% of the stream discharge (QtUs%).

Table 5. Summary table of tracer tests results with fluorescein (Test 1 in July 2011, Test 2 in September 2011, and Test 3 in November 2011).

PARAMETER	TEST 1	TEST 2	TEST 3
Qs = Montellina Spring discharge (L/s)	181.0	144.0	171.0
Mr = mass of fluorescein Mr which had reached the spring (g)	38.086	281.827	123.806
QtUs = Amount of water of low Renanchio Stream that feeds MS (L/s)	14.4	18.7	14.8
QtUs% = percentage of water of low Renanchio Stream that arrives to MS (%)	0.97	14.1	4.2
Qs% = percentage of MS discharge derived from low Renanchio Stream discharge (%)	7.9	13.0	8.7

Consequently, the percentage of MS discharge that is directly derived from the low and middle Renanchio Stream discharge (Qs%) is 7.9%.

The first tracer arrival in Test 2 was recorded at 29 h, but the peak was not measured until 132 h after the injection. The recorded peak concentration was 1.45 µg/L. A detectable concentration was measured for a period of more than 50 days. The mass of fluorescein that reached MS was 281.827 g. This value was used to evaluate QtUs (18.7 L/s), QtUs% (14.1%), and Qs% (13%).

The first fluorescein arrival at spring in Test 3 occurred 23 h after injection. The fluorescein peak (0.78 µg/L) was registered at 72 h after injection, whereas the fluorescein concentration was registered for 35 days after the injection. The value of Mr calculated for this test was 123.806 g. Consequently, the water amount from the low and middle Renanchio Stream that fed MS was 14.8 L/s, which corresponds to 4.2% of the Renanchio Stream discharge. The percentage of MS discharge that was derived from the Renanchio Stream discharge (Qs%) was 8.7% (Table 5).

Tracer tests, analysed as a whole, highlight that only up to 13% of MS discharge is directly fed by the low and middle Renanchio Stream. This percentage corresponds to a discharge between 14.4 L/s and 18.7 L/s, depending on the measurement period. In detail, the first arrival of the tracer to spring in a few hours indicates a fast water flow through open and persistent NE-SW oriented fractures located in sector 2 (Figure 9). The following arrival that reaches spring (up to 50 days) indicates a slower water flow mainly through a fracture network with a lower permeability. The remaining 87% of the spring discharge is not directly fed by the analysed low and medium Renanchio Stream and is, instead, essentially fed from the effective infiltration in the Renanchio Basin, characterized by very fractured rocks, with high permeability, and glacial marginal sediments (see Figure 5).

Despite the large variation of stream discharge and losses, the discharge of the spring remained fairly steady, ranging between 144 and 181 L/s (Table 5). Thus, only a little fraction of the stream losses, and more specifically, discharge varying between approximately 14 and 19 L/s, moves to the spring, despite the high variability of the Renanchio Stream discharge. The relatively constant water supply by the Renanchio Stream to MS, independently of the watercourse discharge, implies a percentage variation from 1% to 14%, depending on base and flood periods (Figure 9).

5. Discussion

MS, as above reported, is located at 375 m a.s.l. on the western slope of the low Dora Baltea Valley, relatively close to the low Renanchio Stream (400 m north). Moreover, it is located approximately 100 m higher than the valley floor and is characterized by a very high discharge (Figure 1), corresponding to approximately 24% of the effective infiltration in the Renanchio Basin (Figure 2B) (Table 4).

The synthesis of geological and hydrogeological surveys of the investigated area suggests that the presence of MS is strictly connected to the different fracturing degrees of bedrock, consisting of an underlying normal fractured body and an overlying from highly fractured to loosened one, the last of which has a thickness of several tens of metres. The normal fractured body, locally outcropping in sector 1, is characterized by a low to very low permeability ($k < 10^{-6}$ m/s), whereas the loosened body that extensively outcrops in sector 2 (DSGSD) has a high permeability due to fractures (Figure 4) ($k = 10^{-2} \div 10^{-3}$ m/s). The superposition of these two rocky bodies defines a permeability boundary along which the groundwater can preferentially flow. Moreover, the bedrock discontinuities located in sector 2 upstream of MS, consisting of both N100° trend open fractures and trenches, (Figure 5C), and NE-SW minor scarps (open and persistent fractures) (Figure 9), are also significant for the feeding of the spring.

Furthermore, the Quaternary cover also has an important role in the location of MS. Indeed, the thick glacial marginal sediments on the entire sector 3 covering the bedrock (Figure 4), forming a set of large lateral moraines connected to the Renanchio Glacier and characterized by a medium permeability for porosity ($k = 10^{-4} \div 10^{-6}$ m/s depending on the matrix grain size), determine a slow groundwater flow essentially supplied by infiltration in the high Renanchio Basin (Figure 5A). The geological reconstruction also highlights the presence of a buried glacial valley floor (covered by glacial marginal sediments) shaped in the bedrock by the Renanchio Glacier in sector 3, but not present in sector 2 (Figures 5B and 7). Thus, it is possible to hypothesize that this landform conveys the most groundwater contained in the glacial marginal sediments.

The hydrogeological constraints comprise a relatively constant MS water chemistry and temperature, suggesting the presence of a large aquifer hosted in the marginal glacial sediments so as to allow homogenization of the chemical composition of groundwater through the year (Table 2).

Moreover, MS temperature values, which are not very variable over time, suggest a relatively deep groundwater flow circuit, scarcely influenced by seasonal air temperature (Table 3).

Additionally, the greater MS electrical conductivity compared to that of the Renanchio Stream, suggesting a high residence time of MS water in the rocks, supports non-exclusive MS feeding by stream water (Table 2).

Detailed information regarding the feeding of MS is provided by fluorescein tracer tests (Figure 13). The arrival of fluorescein to MS in a short time (first arrival variable between 16 and 29 h after the injection of the tracer) testifies to a fast connection between MS and the low Renanchio Stream, shaped in the bedrock. This fast connection takes place through the DSGSD fractures, essentially using the NE-SW minor scarps. Moreover, the arrival of fluorescein in MS recorded for periods up to 50 days can be due to slower groundwater flow through less open DSGSD fractures. The remaining MS discharge is not directly fed by the low Renanchio Stream and it is likely supplied by the effective infiltration in the Renanchio Basin. More specifically, the results of tracer tests highlight that, despite the fact that low and middle Renanchio Stream losses are very variable (from 389 to 41 L/s) depending on watercourse discharge (Figure 12 and Table 5), only a small part of these losses reaches the spring. Particularly, the results of fluorescein tracer tests indicate that the Renanchio Stream losses contributing to MS discharge are low (about 14–19 L/s corresponding to 8–13% of MS discharge) and approximately constant independently of the watercourse discharge (Figure 9 and Table 5).

A hydrogeological conceptual model of the investigated area was therefore reconstructed, summarizing the different geological and hydrogeological data (Figure 5). Groundwater, coming from the effective infiltration of rain and snow in the entire Renanchio Basin, flows in the highly fractured bedrock of sector 4 and in the glacial marginal sediments of sector 3. A large aquifer is located in this last sector, allowing homogenization of the chemical composition of groundwater, with a relatively deep flow circuit, as suggested by the small variability of MS temperature values. In this aquifer, groundwater is characterized by a slow flow velocity and it is then conveyed along the buried glacial valley (Figure 5A,B).

It is possible to assume that the groundwater flow continues through the loosened bedrock outcropping in sector 2 (DSGSD) (Figure 5A,C). Here, the superposition of two rocky bodies with different fracture degrees (normally fractured and loosened bedrock) can favor the groundwater flow along the permeability boundary. In detail, MS is located in correspondence of the ground surface intersection with the permeability boundary. The N100° open fractures and trenches, particularly diffused upstream of MS and facing the spring, are responsible for a significant groundwater flow towards the MS.

At last, only a small part of MS discharge is fed by the low Renanchio Stream, as highlighted by tracer tests. Particularly, groundwater flows from the low Renanchio Stream to MS essentially using open and persistent fractures (NE-SW minor scarps) in the bedrock (Figure 9).

Finally, the HCO_3^- content and the relatively high correlation between HCO_3^- and Ca^{2+} plus the Mg^{2+} content of MS water evidence the presence of dolomitic marble levels in the bedrock. However, these partially karstified marble levels (microkarst), multiple metres thick, furnish a little flow to the spring because (i) the amount of water hosted in these karstified marble levels cannot justify the high discharge of the spring; (ii) the presence of only microkarst can cause a high velocity of groundwater flow, with spring discharge closely dependent on the precipitation, in contrast to the continuous MS discharge; and (iii) the presence of a DSGSD does not allow the maintenance of the continuity of the karst circuit.

6. Conclusion

The research conducted in the low Dora Baltea Valley showed that the occurrence of MS with very high, anomalous, discharge was only partially connected to the low and medium Renanchio Stream, so a more complex solution of the hydrogeological setting was needed. More specifically, the location of MS near the contact between normally fissured bedrock at the base of the slope (sector 1) and loosened

rocks, which form the slope immediately upstream of the spring (sector 2), confirmed an origin partly related to this limit (Figure 5). In detail, MS originates from the coexistence of three main factors, namely, highly fractured bedrock connected to DSGSD, wide and thick glacial sediment cover, and a buried glacial valley, which also drains the high Renanchio Basin (Figure 5). Consequently, MS is a fine example of combined slow flow into glacial sediments and more fast flow through open bedrock fractures, which ensures a reliable water supply for inhabitants.

This investigation, using a multidisciplinary approach with geological and hydrogeological surveys, provides a basis for a methodological approach to define the hydric availability in other alpine springs in the DSGSD context. Considering that large water reservoirs are usually associated with alpine areas characterized by DSGSD, this context can be very favorable for storing large volumes of water, favored by a high infiltration in the open fractures of very thick bodies of loosened bedrock. Furthermore, a wide distribution and a great thickness of glacial sediments, with medium permeability, generally occurs in DSGSD areas and is also promoted by the strong fracturing of bedrock. These sediments, in addition to being a reservoir, are characterized by slow flow, which favors a relatively constant discharge of the springs.

Numerous springs in the alpine area are favored by highly fractured bedrock and a wide distribution of Quaternary sediments. A more sustainable exploitation of the water resource, essentially hosted in rocky masses involved in DSGSD, can greatly help the mountain population support. Many activities (agricultural, farming, touristic including winter sports) that formerly required a small water supply, now show a sharp increase in water needs (i.e., all new plants are made with irrigation systems).

Author Contributions: D.A.D.L., M.L., M.G., M.G.F. and F.G. performed data acquisition. M.L., M.G. and M.G.F. performed data analysis, interpretation and wrote the manuscript. F.G., E.C.A. and D.A.D.L. participated in data analyses and interpretation and contributed to writing the text. M.L. and M.G.F. reviewed the manuscript. D.A.D.L. supervised the work.

Conflicts of Interest: The authors declare no conflict of interest.

References

1. De Luca, D.A.; Masciocco, L.; Caviglia, C.; Destefanis, E.; Forno, M.G.; Fratianni, S.; Gattiglio, M.; Lasagna, M.; Gianotti, F.; Latagliata, V.; et al. Distribution, discharge, geological and physical-chemical features of the springs in the Turin Province (Piedmont, NW Italy). In *Engineering Geology for Society and Territory*; Springer: Berlin/Heldelberg, Germany, 2015; Volume 3, pp. 253–256. [CrossRef]
2. Banzato, C.; Governa, M.; Petricig, M.; Vigna, B. The importance of monitoring for the determination of aquifer vulnerability and spring protection areas. In *Engineering Geology for Society and Territory*; Springer: Berlin/Heldelberg, Germany, 2015; Volume 5, pp. 1379–1385.
3. Binet, S.; Spadini, L.; Bertrand, C.; Guglielmi, Y.; Mudry, J.; Scavia, C. Variability of the groundwater sulfate concentration in fractured rock slopes: A tool to identify active unstable areas. *Hydrol. Earth Sys. Sci. Discuss.* **2009**, *13*, 2315–2327. [CrossRef]
4. Ostermann, M.; Koltai, G.; Spötl, C.; Cheng, H. Deep-seated gravitational slope deformations in the Vinschgau (northern Italy) and their association with springs and speleothems. In Proceedings of the EGU General Assembly Conference Abstracts, Vienna, Austria, 17–22 April 2016.
5. Forno, M.G.; Comina, C.; Gattiglio, M.; Gianotti, F.; Lo Russo, S.; Sambuelli, L.; Raiteri, L.; Taddia, G. Preservation of Quaternary sediments in DSGSD environment: The Mont Fallére case study (Aosta Valley, NW Italy). *Alp. Mediterr. Quat.* **2016**, *29*, 1–11.
6. Madritsch, H.; Millen, B.M.J. Hydrogeologic evidence for a continuous basal shear zone within a deep-seated gravitational slope deformation (Eastern Alps, Tyrol, Austria). *Landslides* **2007**, *4*, 149–162. [CrossRef]
7. Pergher, L.; Burger, U. Measurement of the physical properties of spring water—An easy an efficient tool for the process analysis of mass movements. In Proceedings of the 10th Interpraevent Congress, Riva del Garda, Italy, 24–27 May 2005.

8. Compagnoni, R.; Dal Piaz, G.V.; Hunziker, J.C.; Lombardo, B.; Williams, P.F. The Sesia-Lanzo Zone, a slice of continental crust with alpine high pressure-low temperature assemblages in the Western Italian Alps. *Rend. Soc. It. Mineral. Petrog.* **1977**, *33*, 281–334.
9. Regis, D.; Venturini, G.; Engi, M. Geology of the Scalaro Valley-Sesia Zone (Italian Western Alps). *J. Maps* **2016**, *12*, 621–629. [CrossRef]
10. Venturini, G. Geology, geochemistry and geochronology of the inner central Sesia Zone (Western Alps, Italy). *Mém. Géol. Lausanne* **1995**, *25*, 1–148.
11. Rocco, R.; Santelli, E. Water Resources Management in Valle d'Aosta (Northwest of Italy). *AQUA Mundi* **2010**, *Am01013*, 93–100. [CrossRef]
12. Stefania, G.A.; Rotiroti, M.; Fumagalli, L.; Zanotti, C.; Bonomi, T. Numerical Modeling of Remediation Scenarios of a Groundwater Cr(VI) Plume in an Alpine Valley Aquifer. *Geosciences* **2018**, *8*, 209. [CrossRef]
13. De Luca, D.A.; Destefanis, E.; Forno, M.G.; Lasagna, M.; Masciocco, L. The genesis and the hydrogeological features of the Turin Po Plain fontanili, typical lowland springs in Northern Italy. *Bull. Eng. Geol. Environ.* **2014**, *73*, 409–427. [CrossRef]
14. De Luca, D.A.; Dell'Orto, V.; Destefanis, E.; Forno, M.G.; Lasagna, M.; Masciocco, L. Hydrogeological structure of the "fontanili" in Turin Plain. *Rend. Onl. Soc. Geol. It.* **2009**, *6*, 199–200.
15. Perello, P. Derivazione a Scopi Idroelettrici del Torrente Renanchio. Studio Idrogeologico per la Sorgente Montellina; SEA Consulting srl & GDP. 2010; Unpublished work.
16. Di Gioia, M. Studio Idrogeologico circa i Rapporti tra il Torrente Renanchio e la Sorgente Montellina. 2012; Unpublished report.
17. Piper, A.M. A graphic procedure in the chemical interpretation of water analysis. *Am. Geophys. Un. Trans.* **1944**, *25*, 914–923. [CrossRef]
18. Turc, L. Water requirements assessment of irrigation, potential evapotranspiration: Simplified and updated climatic formula. *Ann. Agron.* **1961**, *12*, 13–49.
19. Celico, P. *Prospezioni Idrogeologiche II*; Liguori Editore: Napoli, Italy, 1988.
20. Kalbus, E.; Reinstorf, F.; Schirmer, M. Measuring methods for groundwater-surface water interactions: A review. *Hydrol. Earth Syst. Sci.* **2006**, *10*, 873–887. [CrossRef]
21. Carter, R.W.; Davidian, J. General procedures for gaging streams. In *Techniques of Water Resources Investigations*; US Geological Survey: Denver, CO, USA, 2009; Book 3, Chapter A-14.
22. Kilpatrick, F.A.; Schneider, V.R. Use of flumes in measuring discharge. In *Techniques of Water-Resources Investigations*; US Geological Survey: Denver, CO, USA, 1983.
23. Rantz, S.E. *Measurement and Computation of Streamflow: Volume 1. Measurement of Stage and Discharge*; US Geological Survey Water-Supply Paper; US Department of the Interior, US Government Printing Office: Washington, DC, USA, 1982; Volume 2175.
24. Kilpatrick, F.A.; Cobb, E.D. Measurement of discharge using tracers. In *Techniques of Water-Resources Investigations*; US Geological Survey: Denver, CO, USA, 1985; Book 3, Chapter A-16.
25. Moore, R.D. Introduction to salt dilution gauging for streamflow measurement: Part I. *Streaml. Water. Manage. Bull.* **2004**, *7*, 20–23.
26. Radulović, M.; Radojević, D.; Dević, D.; Blečić, M. Discharge calculation of the spring using salt dilution method. Application site Bolje Sestre Spring (Montenegro). In Proceedings of the BALWOIS 2008, Ohrid, Republic of Macedonia, 27–31 May 2008.
27. Moore, R.D. Slug injection using salt in solution. *Streaml. Water. Manag. Bull.* **2005**, *8*, 1–6.
28. Wood, P.J.; Dykes, A.P. The use of salt dilution gauging techniques: Ecological considerations and insights. *Wat. Res.* **2002**, *36*, 3054–3062. [CrossRef]
29. Drost, J.W. Single-well and multi-well nuclear tracer techniques-a critical review. In *Technical Documents in Hydrology*; UNESCO: Paris, France, 1989.
30. Zellweger, G.W. Testing and comparison of four ionic tracers to measure stream flow loss by multiple tracer injection. *Hydrol. Process.* **1994**, *8*, 155–165. [CrossRef]
31. Kumar, B.; Nachiappan, R.P. Estimation of alluvial aquifer parameters by a single-well dilution technique using isotopic and chemical tracers: A comparison. In *Tracers and Modelling in Hydrogeology*; Dassargues, A., Ed.; IAHS Press, IAHS Publ.: Wallingford, UK, 2000; Volume 262, pp. 53–56.
32. Tazioli, A. Experimental methods for river discharge measurements: Comparison among tracers and current meter. *Hydrol. Sci. J.* **2011**, *56*, 1314–1324. [CrossRef]

33. Comina, C.; Lasagna, M.; De Luca, D.A.; Sambuelli, L. Geophysical methods to support correct water sampling locations for salt dilution gauging. *Hydrol. Earth Syst. Sci.* **2014**, *18*, 3195–3203. [CrossRef]
34. Gees, A. Flow measurement under difficult measuring conditions: Field experience with the salt dilution method. In *Hydrology in Mountainous Regions*; IAHS Publication: Wallinford, UK, 1990; Volume 193, pp. 255–262.
35. Käss, W. *Tracing Technique in Geohydrology*; Balkema: Rotterdam, The Netherlands, 1998.
36. Taylor, C.J.; Greene, E.A. Hydrogeologic characterization and methods used in the investigation of karst hydrology. In *Field Techniques for Estimating Water Fluxes between Surface Water and Ground Water*; Rosenberry, D.O., La Baugh, J.W., Eds.; US Geological Survey: Denver, CO, USA, 2008.
37. Clemente, P.; Lasagna, M.; Dino, G.A.; De Luca, D.A. Comparison of different methods for detecting irrigation canals leakage. In *Engineering Geology for Society and Territory*; Lollino, G., Arattano, M., Rinaldi, M., Giustolisi, O., Marechal, J.C., Grant, G.E., Eds.; Springer: Berlin/Heldelberg, Germany, 2015; Volume 3, pp. 23–26. [CrossRef]
38. Aldous, P.J.; Fawell, J.K. *The Use of Fluorescein Sodium (Uranine) for Groundwater Tracing Investigations in Potable Water Supplies*; WRc Environment, Medmenham Lab.: Medmenham Bucks, UK, 1986.
39. Field, M.S.; Wilhelm, R.G.; Quinlan, J.F.; Aley, T.J. An assessment of the potential adverse properties of fluorescent tracer dyes used for groundwater tracing. *Environ. Monit. Ass.* **1995**, *38*, 75–96. [CrossRef]
40. Behrens, H.; Beims, U.; Dieter, H.; Dietze, G.; Eikmann, T.; Grummt, T.; Hanisch, H.; Henseling, H.; Kaess, W.; Kerndorff, H.; et al. Toxicological and ecotoxicological assessment of water tracers. *Hydrogeol. J.* **2001**, *9*, 321–325. [CrossRef]
41. Hart, S.R.; Staudigel, H.; Workman, R.; Koppers, A.A.P.; Girard, A.P. A fluorescein tracer release experiment in the hydrothermally active crater of Vailulu'u volcano, Samoa. *J. Geophys. Res.* **2003**, *108*, 2377. [CrossRef]
42. Buzády, A.; Erostyák, J.; Paàl, G. Determination of uranine tracer dye from underground water of Mecsek Hill, Hungary. *J. Biochem. Biophys. Meth.* **2009**, *69*, 207–214. [CrossRef]
43. Rowinski, P.M.; Chrzanowski, M. Influence of selected fluorescent dyes on small aquatic organisms. *Act. Geophys.* **2010**, *59*, 91–109. [CrossRef]
44. Kasnavia, T.; Vu, D.; Sabatini, D.A. Fluorescent dye and media properties affecting sorption and tracer selection. *Groundwater* **1999**, *37*, 376–381. [CrossRef]
45. Smart, C.C.; Zabo, L.; Alexander, E.C., Jr.; Worthington, S.R.H. Some advances in fluorometric techniques for water tracing. *Environ. Monit. Assess.* **1998**, *53*, 305–320. [CrossRef]
46. Field, M.S. Quantitative analysis of tracer breakthrough curves from tracing tests in karst aquifers. In *Karst Modelling*; Palmer, A.N., Palmer, M.V., Sasowsky, I.D., Eds.; Karst Waters Institute Special Publication: Leesburg, VA, USA, 1999; Volume 5, pp. 163–171.
47. Mull, D.S.; Smoot, J.L.; Liebermann, T.D. Dye tracing techniques used to determine ground-water flow in a carbonate aquifer system near Elizabethtown, Kentucky. In *Water-Resources Investigations Report*; US Geological Survey: Denver, CO, USA, 1988; pp. 1–95.
48. Gospodaric, R.; Habic, P. *Underground water tracing-Investigations in Slovenia, 1972–1975*; Postojna Inst. for Karts Research SAZU: Postojna, Yugoslavia, 1976; pp. 1–305.
49. Wright, W.G.; Moore, B. *Application of Tracer-Injection Techniques to Demonstrate Surface-Water and Ground-Water Interactions between an Alpine Stream and the North Star Mine, Upper Animas River Watershed, Southwestern Colorado*; U.S. Department of the Interior, U.S. Geological Survey: Reston, VA, USA, 2003.
50. Schnegg, P.A. An inexpensive field fluorometer for hydrogeological tracer tests with three tracers and turbidity measurement. In Proceedings of the 22th IAH and ALHSUD Congress on Groundwater and Human Development, Mar del Plata, Argentina, 21–25 October 2002; Bocanegra, E., Martinez, D., Massone, H., Eds.; pp. 1484–1488.
51. Schnegg, P.A. A new field fluorometer for multi-tracer tests and turbidity measurement applied to hydro-geological problems. In Proceedings of the 8th International Congress of the Brazilian Geophysical Society, Rio de Janeiro, Brazil, 14–18 September 2003.

52. Poulain, A.; Rochez, G.; Van Roy, J.P.; Dewaide, L.; Hallet, V.; De Sadelaer, G. A compact field fluorometer and its application to dye tracing in karst environments. *Hydrogeol. J.* **2017**, *25*, 1517–1524. [CrossRef]
53. Field, M.S. *The QTRACER2 Program for Tracer-Breakthrough Curve Analysis for Tracer Tests in Karstic Aquifers and Other Hydrologic Systems*; US Environmental Protection Agency: Washington, DC, USA, 2002; pp. 1–179.